Available online at www.sciencedirect.com
SCIENCE DIRECT®
Advances in Water Resources 26 (2003) 747–757
Advances in Water Resources
www.elsevier.com/locate/advwatres

A new closed-form solution for a radial two-layer drawdown equation for groundwater under constant-flux pumping in a finite-radius well

Hund-Der Yeh [a,*], Shaw-Yang Yang [b], Huan-Yi Peng [a]

[a] Institute of Environmental Engineering, National Chiao-Tung University, No. 75 Po-Ai Street, Hsinchu 300, Taiwan
[b] Department of Civil Engineering, Van-Nung Institute of Technology, Chungli 320, Taiwan

Received 9 November 2002; received in revised form 14 March 2003; accepted 15 March 2003

Abstract

A mathematical model is presented for describing the groundwater flow in a radial two-layer confined aquifer system with a constant-flux pumping well that has a wellbore skin and finite well radius. The Laplace-domain solution for the model is first derived by the Laplace transforms; and the time-domain solution in terms of the aquifer drawdown is then obtained form the Laplace inversion using the Bromwich integral method. When neglecting the well radius, our Laplace-domain solution is shown to reduce to a Laplace-domain solution given by Butler [J. Hydrol. 101 (1988) 15]. A unified numerical approach including a root search approach, the Gaussian quadrature, and the Shanks method is employed for evaluating this time-domain solution. The evaluated results of the solution agree well with those of the Laplace-domain solution estimated by the modified Crump algorithm. This new solution can be used either to predict the spatial and temporal drawdown distributions in both the skin and formation zones or to investigate the effects of the skin type, skin thickness and well radius on the drawdown distribution.

Keywords: Pumping test; Confined aquifer; Closed-form solution; Numerical method; Laplace transforms; Wellbore skin

1. Introduction

The constant-flux test can be employed to determine the in situ hydraulic properties of soil and rock formations, during which, the well discharge (or injection) rate is maintained at a constant value. The resulting measured drawdown data from the observation wells can be used to determine the aquifer parameters, i.e., transmissivity and storage coefficient. Several previous researchers have discussed such problems in a single-layer aquifer system (called a uniform aquifer system) and provided the mathematical models or results for engineering applications. The studies published in the areas of petroleum engineering, heat conduction, and groundwater hydraulics may be classified into two types. One type neglects the well radius, considering the well as a point source (e.g., [28]). Based on this assumption, Streltsova and McKinley [26] discussed the drawdown or buildup calculations for a well in a reservoir with various heterogeneous properties, mostly dealing with no-flow and constant pressure boundaries. However, in reality the radius of pumping well is nonzero; thus, this assumption may lead to some error in data analyses [20]. The other type of study deals with a finite-radius well which is subject to a constant-flux pumping (e.g., [11,14,15,25]). Carslaw and Jaeger [1940, reported by Jaeger, 17] derived a closed-form solution for a heat conduction problem by using the Laplace transforms and a contour integral method. Their solution for temperature distribution in an infinite medium was expressed in an integral form that covers a range from zero to infinity and has an integrand comprised of the product and the square of the Bessel functions. Tabular values estimated by the various approximate formulas were given by Ingersoll et al. [14,15] for dimensionless temperature change versus dimensionless time and by Hantush [11] for dimensionless drawdown versus dimensionless time at dimensionless distances of 1, 2, 5 and 10. Papadopulos and Cooper [22] presented a closed-form solution for the drawdown in a large-diameter

* Corresponding author. Tel.: +886-3-573-1910; fax: +886-3-572-6050.
E-mail address: hdyeh@mail.nctu.edu.tw (H.-D. Yeh).

0309-1708/03/$ - see front matter
doi:10.1016/S0309-1708(03)00046-0

well which accounts for the effect of well storage. A set of type curves evaluated from their solution provides a useful tool to analyze pumping-test data for the aquifer parameters. Their solution can be closely approximated by the Theis solution for small well radius and/or large aquifer transmissivity [7]. Streltsova [25] also evaluated the numerical values for dimensionless drawdown at the well as a function of dimensionless time, giving the results in tabular form.

In addition, a finite thickness of wellbore skin may develop during the well constructions as a result of drilling through a mud or the extensive well development. Consequently, a uniform aquifer may then have a skin zone near the well and become a radial two-layer system (also called a composite system). This skin zone may affect the drawdown of pumping, with the magnitude of the drawdown depending on the thickness and permeability contrast between the skin and the formation. The well drilling causes an invasion of drilling mud into the aquifer and may produce a positive wellbore skin (also called positive skin [20] or low-conductivity skin) that has lower permeability than that of the original formation. In contrast, extensive well development and/or substantial spalling and fracturing of the borehole wall may increase the permeability of the adjacent formation around the well. Under such circumstances, the disturbed formation is referred to as a negative wellbore skin (also called negative skin [20] or high-conductivity skin). Furthermore, geochemical precipitation or dissolution around the well may also respectively reduce or enhance the skin permeability. In any case, the thickness of the skin zone may range from a few millimeters to several meters and thus must be considered in pumping-test data analyses [20]. Barker and Herbert [2] considered a problem for a constant-rate pumping at a well situated at the center of a disc of anomalous transmissivity and storage coefficient in an aquifer which is called a patchy aquifer. The radius of the disc may be of 60 m, and such a patchy aquifer can also be treated as a two-layer aquifer system.

The effects of the well storage as well as the wellbore skin on the results of pumping tests have been investigated in the petroleum industry (e.g., [3,8,18]) and the groundwater hydraulics (e.g., [2,4]). The solutions are available for the aquifer system accounting for the well storage and the infinitesimally small well radius of the pumping well. Barker and Herbert [2] and Butler [4] presented a Laplace-domain solution for the transient, pumping-induced drawdown without considering the well radius. In addition, Barker and Herbert [2] also explicitly derived Jacob's drawdown equation from their Laplace-domain solution at long-time condition. Wikramaratna [29] developed a closed-form solution for describing an abstraction from a vertical multiple-layer confined aquifer with no cross flow when applying Papadopulos and Cooper's solution [22]. His solution takes account of well storage, so the solution can be applied both to large- and small-diameter wells. Novakowski [20] presented a composite analytical solution for a radial two-layer system using the Laplace transform method, producing type curves by using the numerical inversion from the Laplace-domain solution. These type curves were used to interpret the effects of the well storage and the finite-thickness skin on the pumping-test data. Novakowski [21] also reviewed the Laplace-domain solutions, which account for the effects of well storage and finite-thickness skin for the slug and pumping tests, and also provided a computer program which can generate data for the type curves. Hemker [12] presented an integration of both analytical and numerical techniques to find a solution for the general problem of computing well flow in vertically heterogeneous aquifers. Lebbe [19] proposed a unique and generalized interpretation method for single and multiple pumping tests made in an aquifer with layered heterogeneity and with or without lateral anisotropy. Butler and Liu [5] presented an analytical solution for drawdown due to pumping in a uniform aquifer (single-layer system), which contains an arbitrarily located disk of anomalous properties. The well diameter is assumed to be infinitesimally small, i.e., the well is considered as a point source. So far, the existing solutions for composite models in a radial two-layer confined aquifer system under constant-flux pumping are only in the Laplace domain, and the time-domain results are obtained with resort to numerical inversions. None of the existing solutions is to present a closed-form solution in the time domain for such a radial two-layer system.

Although the Laplace-domain solutions are capable of plotting type curves; yet the accuracy of the results obtained from numerical inversions may be unknown or even poor in some cases. The time-domain solution is especially useful in cases like parameter identification as well as verification for numerical models, where the Laplace-domain solution may be of limited or no use. The objectives of this paper are to derive a new time-domain solution for the drawdown distribution in a radial two-layer aquifer system with a finite-radius and constant-flux pumping well and to provide an efficient numerical approach for evaluating the solution (dimensionless drawdown) at specified dimensionless time and distance. The derived solution is in terms of an integral that covers a range from zero to infinity and has an integrand comprising many product terms of the Bessel functions of the first and second kinds of zero and first orders. The numerical approach, including a root search scheme, a numerical integration method, and the Shanks method, is proposed to evaluate the time-domain solution. This solution can be used to investigate the effects of the skin type, the skin thickness, and the well radius on the drawdown distribution in a radial two-layer confined aquifer system.

2. Mathematical model

2.1. Radial two-layer drawdown equation

Several assumptions made for modeling the aquifer system are: (1) the aquifer is homogeneous, isotropic, and infinite-extent with a constant thickness; (2) the well is fully penetrated and with a finite radius; (3) the pumping rate is maintained at a constant value throughout the whole test period; and (4) the skin is a finite thickness near the well. Fig. 1 depicts the well with a constant pumping rate and the cross-section configurations in a radial two-layer confined aquifer system. The governing equations describing the drawdowns, s (or $s(r,t)$), in the skin and formation zones are, respectively,

$$\frac{\partial^2 s_1}{\partial r^2}+\frac{1}{r}\frac{\partial s_1}{\partial r}=\frac{S_1}{T_1}\frac{\partial s_1}{\partial t},\quad r_w \leqq r \leqq r_1 \tag{1}$$

and

$$\frac{\partial^2 s_2}{\partial r^2}+\frac{1}{r}\frac{\partial s_2}{\partial r}=\frac{S_2}{T_2}\frac{\partial s_2}{\partial t},\quad r_1 \leqq r < \infty \tag{2}$$

where subscripts 1 and 2 respectively denote the skin and formation zones, and t is the time from the start of the test. The variable r is the radial distance from the centerline of the well, r_w is the radius of the well, and r_1 is the radial distance from the centerline of the well to the outer skin envelope (or the radius of the disc of the patchy aquifer). Parameters T and S are respectively the transmissivity and the storage coefficient.

The drawdown is initially equal to zero in both the skin and the formation. Thus, the initial conditions for Eqs. (1) and (2) may be written as

$$s_1(r,0)=s_2(r,0)=0 \tag{3}$$

The drawdown tends to zero as r approaches infinity. Therefore, the outer boundary condition for the formation may be specified as

$$s_2(\infty,t)=0 \tag{4}$$

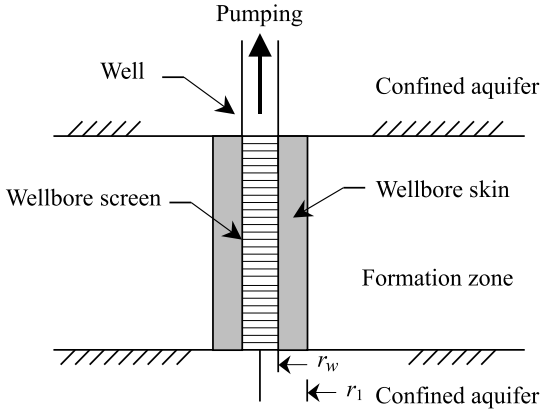

Fig. 1. The well and aquifer configurations.

Using the Darcy law, the boundary condition for maintaining a constant flux across the well is expressed as

$$-\left.\frac{\partial s}{\partial r}\right|_{r=r_w}=\frac{Q}{2\pi r_w T_1},\quad t>0 \tag{5}$$

where Q is a constant-pumping rate. Note that a term representing the rate of decrease in the volume of water within the well should be added to the left-hand-side of Eq. (5) if the effect of the wellbore storage is to be considered [22].

Finally, the continuities of the drawdown and the flow rate between the skin and the formation require that

$$s_1(r_1,t)=s_2(r_1,t),\quad t>0 \tag{6}$$

and

$$T_1\frac{\partial s_1(r_1,t)}{\partial r}=T_2\frac{\partial s_2(r_1,t)}{\partial r},\quad t>0 \tag{7}$$

2.2. Laplace-domain solution

The Laplace transforms [13] are applied to the governing equations and the boundary conditions for the drawdown distributions in the skin and the formation. The results of the Laplace-domain solution $\bar{s}$ are respectively

$$\bar{s}_1=\frac{Q}{4\pi T_2}\left[\frac{1}{p}\frac{2T_2}{r_w T_1 q_1}\frac{\Phi_2 K_0(q_1 r)+\Phi_1 I_0(q_1 r)}{\Phi_2 K_1(q_1 r_w)-\Phi_1 I_1(q_1 r_w)}\right] \tag{8}$$

and

$$\bar{s}_2=\frac{Q}{4\pi T_2}\left[\frac{1}{p}\frac{2T_2}{r_w T_1 q_1}\frac{(\Phi_2 K_0(q_1 r_1)+\Phi_1 I_0(q_1 r_1))K_0(q_2 r)}{(\Phi_2 K_1(q_1 r_w)-\Phi_1 I_1(q_1 r_w))K_0(q_2 r_1)}\right] \tag{9}$$

where $q_1^2=pS_1/T_1$, $q_2^2=pS_2/T_2$, and p is the Laplace variable. The notations $I_0(\cdot)$ and $K_0(\cdot)$ are respectively the modified Bessel functions of the first and second kinds of order zero, and $I_1(\cdot)$ and $K_1(\cdot)$ are respectively the modified Bessel functions of the first and second kinds of order first. Variables Φ_1 and Φ_2 are respectively defined as

$$\Phi_1=K_1(q_1 r_1)K_0(q_2 r_1)-\sqrt{\frac{S_2 T_2}{S_1 T_1}}K_0(q_1 r_1)K_1(q_2 r_1) \tag{10}$$

and

$$\Phi_2=I_1(q_1 r_1)K_0(q_2 r_1)+\sqrt{\frac{S_2 T_2}{S_1 T_1}}I_0(q_1 r_1)K_1(q_2 r_1) \tag{11}$$

Note that Eqs. (8) and (9) can reduce to the Laplace-domain solutions presented by Butler [4] when neglecting the well radius ($r_w \to 0$) as shown in Appendix A.

2.3. Time-domain solution

The solution of Eq. (8) in the time domain obtained by using the Bromwich integral [13, p. 624] is shown in Appendix B; and the drawdown distribution for the skin zone, s_1 is

$$s_1 = \frac{Q}{4\pi T_2}\left[\frac{4T_2}{\pi r_w T_1}\int_0^\infty (1-e^{-(T_1/S_1)u^2 t}) \times \frac{A_1(u)B_1(u)+A_2(u)B_2(u)}{B_1^2(u)+B_2^2(u)}\frac{du}{u^2}\right] \quad (12)$$

with

$$A_1(u) = [J_1(r_1u)Y_0(\kappa r_1u)Y_0(ru) - Y_1(r_1u)Y_0(\kappa r_1u)J_0(ru)] - \sqrt{\frac{S_2T_2}{S_1T_1}}[J_0(r_1u)Y_1(\kappa r_1u)Y_0(ru) - Y_0(r_1u)Y_1(\kappa r_1u)J_0(ru)] \quad (13)$$

$$A_2(u) = [Y_1(r_1u)J_0(\kappa r_1u)J_0(ru) - J_1(r_1u)J_0(\kappa r_1u)Y_0(ru)] - \sqrt{\frac{S_2T_2}{S_1T_1}}[Y_0(r_1u)J_1(\kappa r_1u)J_0(ru) - J_0(r_1u)J_1(\kappa r_1u)Y_0(ru)] \quad (14)$$

$$B_1(u) = [J_1(r_1u)J_0(\kappa r_1u)Y_1(r_wu) - Y_1(r_1u)J_0(\kappa r_1u)J_1(r_wu)] - \sqrt{\frac{S_2T_2}{S_1T_1}}[J_0(r_1u)J_1(\kappa r_1u)Y_1(r_wu) - Y_0(r_1u)J_1(\kappa r_1u)J_1(r_wu)] \quad (15)$$

and

$$B_2(u) = [J_1(r_1u)Y_0(\kappa r_1u)Y_1(r_wu) - Y_1(r_1u)Y_0(\kappa r_1u)J_1(r_wu)] - \sqrt{\frac{S_2T_2}{S_1T_1}}[J_0(r_1u)Y_1(\kappa r_1u)Y_1(r_wu) - Y_0(r_1u)Y_1(\kappa r_1u)J_1(r_wu)] \quad (16)$$

where u is a dummy variable and $\kappa = \sqrt{T_1S_2/T_2S_1}$. Note that $J_0(\cdot)$ and $Y_0(\cdot)$ are respectively the Bessel functions of the first and second kinds of order zero, and $J_1(\cdot)$ and $Y_1(\cdot)$ are respectively the Bessel functions of the first and second kinds of order first.

The drawdown distribution for the formation, s_2, can be obtained in a similar manner as

$$s_2 = \frac{Q}{4\pi T_2}\left[\frac{8T_2}{\pi^2 r_w r_1 T_1}\int_0^\infty (1-e^{-(T_1/S_1)u^2 t}) \times \frac{Y_0(\kappa ru)B_1(u) - J_0(\kappa ru)B_2(u)}{B_1^2(u)+B_2^2(u)}\frac{du}{u^3}\right] \quad (17)$$

Notably, the term inside the bracket of Eq. (12) or (17) can be considered as the well function for a constant pumping from a finite-radius well in a radial two-layer aquifer system.

2.4. Dimensionless solutions

Defining dimensionless variables $\alpha = T_2/T_1$, $\beta = S_2/S_1$, $\tau = T_2t/S_2r_w^2$, $\rho = r/r_w$, $\rho_1 = r_1/r_w$, $\sigma = s(4\pi T_2)/Q$, and $\overline{\sigma} = \bar{s}(4\pi T_2)/Q$. The Laplace-domain solutions for dimensionless drawdown, $\overline{\sigma}$, derived from Eqs. (8) and (9) may be respectively expressed as

$$\overline{\sigma}_1 = \frac{1}{p}\left[\frac{2\alpha}{\sqrt{p}/\kappa}\frac{\phi_2K_0(\sqrt{p}\rho/\kappa)+\phi_1I_0(\sqrt{p}\rho/\kappa)}{\phi_2K_1(\sqrt{p}/\kappa)-\phi_1I_1(\sqrt{p}/\kappa)}\right] \quad (18)$$

and

$$\overline{\sigma}_2 = \frac{1}{p}\left[\frac{2\alpha}{\sqrt{p}/\kappa}\frac{(\phi_2K_0(\sqrt{p}\rho_1/\kappa)+\phi_1I_0(\sqrt{p}\rho_1/\kappa))K_0(\sqrt{p}\rho)}{(\phi_2K_1(\sqrt{p}/\kappa)-\phi_1I_1(\sqrt{p}/\kappa))K_0(\sqrt{p}\rho_1)}\right] \quad (19)$$

where

$$\phi_1 = K_1(\sqrt{p}\rho_1/\kappa)K_0(\sqrt{p}\rho_1) - \sqrt{\frac{S_2T_2}{S_1T_1}}K_0(\sqrt{p}\rho_1/\kappa)K_1(\sqrt{p}\rho_1) \quad (20)$$

and

$$\phi_2 = I_1(\sqrt{p}\rho_1/\kappa)K_0(\sqrt{p}\rho_1) + \sqrt{\frac{S_2T_2}{S_1T_1}}I_0(\sqrt{p}\rho_1/\kappa)K_1(\sqrt{p}\rho_1) \quad (21)$$

Accordingly, the dimensionless-drawdown solutions, σ, derived from Eqs. (12) and (17) are respectively

$$\sigma_1 = \frac{4\alpha}{\pi}\int_0^\infty (1-e^{-\beta\tau w^2/\alpha}) \times \frac{[A_1(w)B_1(w)+A_2(w)B_2(w)]}{[B_1^2(w)+B_2^2(w)]}\frac{dw}{w^2} \quad (22)$$

and

$$\sigma_2 = \frac{8\alpha}{\pi^2\rho_1}\int_0^\infty (1-e^{-\beta\tau w^2/\alpha}) \times \frac{[Y_0(\kappa\rho w)B_1(w) - J_0(\kappa\rho w)B_2(w)]}{[B_1^2(w)+B_2^2(w)]}\frac{dw}{w^3} \quad (23)$$

where $w = r_wu$,

$$A_1(w) = [J_1(\rho_1w)Y_0(\kappa\rho_1w)Y_0(\rho w) - Y_1(\rho_1w)Y_0(\kappa\rho_1w)J_0(\rho w)] - \sqrt{\alpha\beta}[J_0(\rho_1w) \times Y_1(\kappa\rho_1w)Y_0(\rho w) - Y_0(\rho_1w)Y_1(\kappa\rho_1w)J_0(\rho w)] \quad (24)$$

$$A_2(w) = [Y_1(\rho_1w)J_0(\kappa\rho_1w)J_0(\rho w) - J_1(\rho_1w)J_0(\kappa\rho_1w)Y_0(\rho w)] - \sqrt{\alpha\beta}[Y_0(\rho_1w) \times J_1(\kappa\rho_1w)J_0(\rho w) - J_0(\rho_1w)J_1(\kappa\rho_1w)Y_0(\rho w)] \quad (25)$$

$$B_1(w) = [J_1(\rho_1w)J_0(\kappa\rho_1w)Y_1(w) - Y_1(\rho_1w)J_0(\kappa\rho_1w)J_1(w)] - \sqrt{\alpha\beta}[J_0(\rho_1w) \times J_1(\kappa\rho_1w)Y_1(w) - Y_0(\rho_1w)J_1(\kappa\rho_1w)J_1(w)] \quad (26)$$

and

$$B_2(w) = [J_1(\rho_1 w)Y_0(\kappa\rho_1 w)Y_1(w) - Y_1(\rho_1 w)Y_0(\kappa\rho_1 w)J_1(w)] - \sqrt{\alpha\beta}[J_0(\rho_1 w)Y_1(\kappa\rho_1 w)Y_1(w) - Y_0(\rho_1 w)Y_1(\kappa\rho_1 w)J_1(w)] \quad (27)$$

The dimensionless drawdown in a single-layer aquifer system is given as [11,14]

$$\sigma(\rho,\tau) = \frac{4}{\pi}\int_0^\infty (1-\mathrm{e}^{-\tau w^2}) \times \frac{[Y_0(\rho w)J_1(w) - J_0(\rho w)Y_1(w)]}{[J_1^2(w)+Y_1^2(w)]}\frac{\mathrm{d}w}{w^2} \quad (28)$$

If the dimensionless aquifer properties in a radial two-layer aquifer system are assumed to equal unity for each parameter, i.e., $\alpha = \beta = 1$; then, both Eqs. (22) and (23) can reduce to Eq. (28) algebraically.

3. Numerical evaluations

The improper integrals of Eqs. (22) and (23) may be difficult to directly evaluate due to the slow convergence of the Bessel functions and their products. However, the integral may be transformed as a sum of infinite series and each term of the series is obtained by integrating the area under the integrand and between two consecutive roots along the horizontal axis. Thus, these two integrals are evaluated by the proposed approach including a root search scheme, the Gaussian quadrature, and the Shanks method [23]. The root search scheme employs the Newton method to search for the next root if there is only a single-peak wave within any two consecutive roots. On the other hand, a combination of the bisection method and the Newton method is adopted to search for next root when the double-peak wave happens between two consecutive roots. The Gaussian quadrature is used for performing the numerical integration within the chosen interval. The Shanks method is applied to accelerate convergence when evaluating the Bessel functions and the alternating series obtained from evaluating the integral.

3.1. Root search scheme

In the root search scheme, initial guess values are required to find the sequential roots. A reasonable estimate of the increment obtained from the solution of a single-layer system is chosen to approximate the first (none-zero) root of the solution for a two-layer system. The dimensionless distance, ρ, is a critical factor to determine the location of the non-zero roots. For $\rho > 1$, the asymptotic expansion of the large positive ith-root for the bracket term on the right-hand-side (RHS) of Eq. (28), w_i, is [1, p. 374]

$$w_i = c + \frac{d}{c} + \frac{e-d^2}{c^3} + \cdots, \quad i = 1,2,\ldots,n \quad (29)$$

where $c = (i-1/2)\pi/(\rho-1)$, $d = (3\rho+1)/[8\rho(\rho-1)]$, and $e = (-63\rho^3-25)/[6(4\rho)^3(\rho-1)]$.

When ρ is small, Eq. (29) gives good approximations for the first few non-zero roots of the integrand of Eq. (28). The interval between the first two roots is approximately equal to $\pi/2(\rho-1)$, which is obtained by simply neglecting the second and remaining terms of Eq. (29). Therefore, the increment Δ_1 from the origin to the first (none-zero) root approximately equals $\pi/2(\rho-1)$. When ρ is large, the approximate result of using the increment Δ_1 to estimate the large roots of the integrand will be very poor; in other words, other increments that give good approximations to the larger roots are needed. As a reasonable guess for the second increment, Δ_2 is chosen to be equal to the first (non-zero) root w_1; thus, the second root w_2 is approximately equal to $2w_1$ Similarly, the remaining increments Δ_i are chosen as $w_{i-1} - w_{i-2}$; and therefore, the remaining roots may be approximately equal to $w_i = w_{i-1} + \Delta_i$ where $i = 3,4,\ldots$.

3.2. Evaluation of integral

Both the six-term and ten-term formulas of the Gaussian quadrature are used together to carry out the numerical integration for the area under the integrand. Starting from the origin, a small step-size, Δw, is chosen for the integration. The integration results after applying the six-term and ten-term formulas are defined as A_6 and A_{10} respectively. The difference of two integration results is defined as $\Delta A = |A_{10} - A_6|$. A half step-size ($\Delta w/2$) will be used if $\Delta A > 10^{-7}$ and the same integration procedure will be repeated again. The same step-size (Δw) is employed if $10^{-8} \leqq \Delta A \leqq 10^{-7}$ and a double step-size ($2\Delta w$) is chosen if $\Delta A < 10^{-8}$ for next integration. This scheme ensures that each integration result over a small step-size is accurate to seven decimal places.

For $\rho = 1$ (i.e., at the rim of the well), the plot of the integrand is a single-peak curve. The initial step-size, Δw, is chosen very small, say 10^{-5}, for the integrand of Eq. (22); then, both the six-term and ten-term formulas of the Gaussian quadrature are used at the same time to carry out the integration. The integration procedure described above is applied to successive integrations from zero to infinity. As long as the result of the integration is less than 10^{-10}, the remaining integration toward infinity is estimated by changing the variable to be $y = 1/w$, and the transformed integral in terms of y is directly evaluated by the Gaussian quadrature [12, p. 304]. Finally, the dimensionless drawdown represented by Eq. (22) for $\rho = 1$ can be obtained by simply adding all the integration results from each small step.

For $\rho > 1$, the curve of the integrand exhibits two peaks within two adjacent roots when the aquifer has a positive skin ($\alpha > 1$), and a single peak when the aquifer has a negative skin ($\alpha < 1$) or uniform formation ($\alpha = 1$). The root search approach is used to find the sequential roots; whereas a combination of the bisection method and the Newton method is adopted if $\alpha > 1$ and the Newton method is adopted for $\alpha \leqq 1$. The initial step-size is chosen to be the half distance between two adjacent roots, i.e., $\Delta w_i = (w_i - w_{i-1})/2$. The proposed integration procedure is applied over the w-axis. Note that the last step-size is chosen such that the end of the last step-size should be located right at the next root. The area between any two adjacent roots, which represents a term of an infinite series, is then obtained by adding the sum of the results obtaining from the integration for each step-size. It should be noted that the integrands of Eqs. (22) and (23) exhibit oscillatory behavior because of the nature of the Bessel functions, so the resultant infinite series may have the problem of slow convergence. Since the Shanks method had been shown to be a very efficient algorithm for accelerating the convergence of a slowly convergent series [23,30], it is employed here to accelerate the convergence in summing the alternating series.

3.3. Numerical inversion

The Laplace-domain solution for mathematical models in many engineering problems may be tractable, yet the corresponding solution in the time domain may not be possible or easily solved. Under such circumstances, methods of numerical Laplace inversion such as the Stehfest algorithm [24], the Talbot method [27], or the Crump algorithm [9] may be used. Herein, the modified Crump algorithm [10,16] is adopted to invert the Laplace-domain solutions (Eqs. (18) and (19)) to an accuracy of five decimal places. Then, the numerical inversion results are compared with the values of the time-domain solution estimated by the proposed approach.

4. Results and discussion

In this section, the dimensionless time–drawdown and distance–drawdown curves are plotted to investigate the influences of various factors on the drawdown distribution for the case of $\rho_1 = 3$. The time-domain solutions of Eqs. (22) and (23) are evaluated by the proposed approach; while the Laplace-domain solutions of Eqs. (18) and (19) are evaluated by the modified Crump algorithm. The double-precision format is used for all evaluations and the convergence criterion for the Shanks method is set as 10^{-7}.

4.1. Comparison of the time-domain solution and inversion from the Laplace-domain solution

Figs. 2 and 3 respectively show the dimensionless time–drawdown and distance–drawdown curves based on the closed-form and Laplace-domain solutions for $\rho = 1$, 3 and 5 when $\alpha = 0.5$, 1 or 2. The formation has a negative skin if $\alpha = 0.5$ and a positive skin if $\alpha = 2$; while the formation has only a single layer for $\alpha = 1$. Notably, the results of the Laplace-domain solution agree very well with those of the closed-form solution as indicated in Figs. 2 and 3. These comparisons may suggest that both solutions are correctly evaluated.

Within the skin zone ($1 \leqq \rho \leqq 3$), Fig. 2 shows that the dimensionless time–drawdown curve for a single-layer formation appears significantly different from that with a positive or negative skin. The well with positive skin produces the largest dimensionless drawdown, the single layer is the second, and the well with negative skin yields the smallest among these three drawdown curves. The positive skin has lower conductivity and requires a larger head loss to maintain the constant flow rate, while the negative skin requires a lower head loss, compared with the solution of a single-layer system. Within the aquifer formation (i.e., $\rho \geqq 3$), the dimensionless drawdown for the system with a positive skin is smaller than

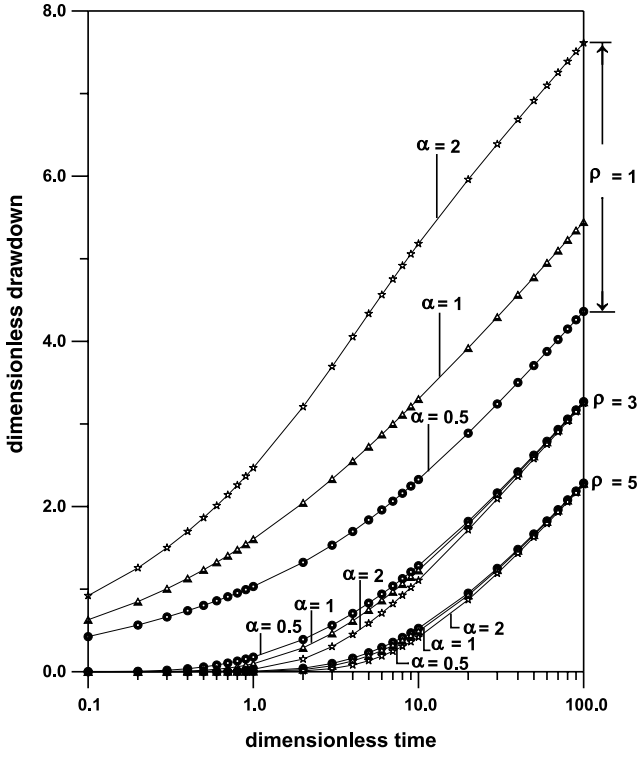

Fig. 2. The time-domain solution evaluated by the proposed approach and the Laplace-domain solution evaluated by the modified Crump algorithm for $\rho = 1$, 3 and 5 while $\alpha = 0.5$, 1 or 2. The solid line represents the time-domain solution, and the symbols ●, ▲ and ★ represent the numerical inversion solutions.

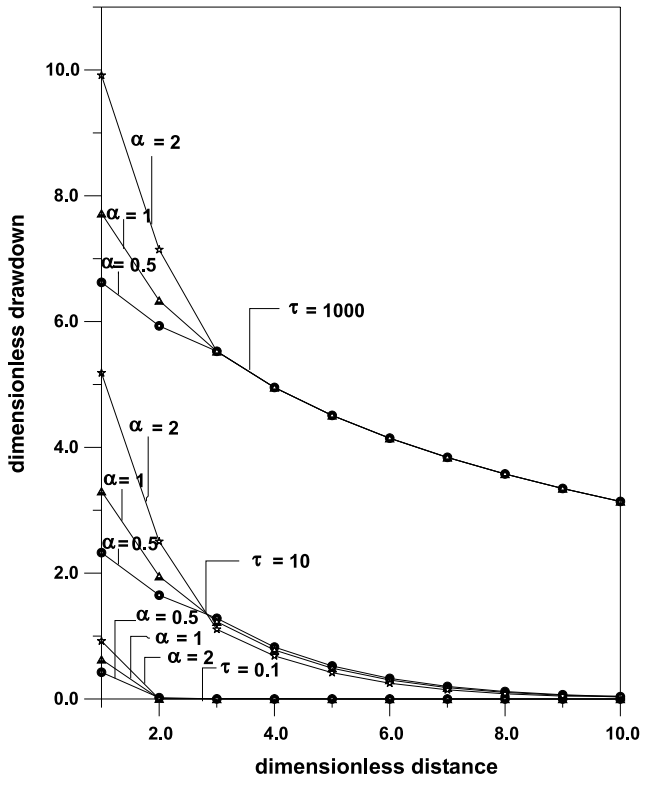

Fig. 3. The time-domain solution evaluated by the proposed approach and the Laplace-domain solution evaluated by the modified Crump algorithm for $\tau = 0.1$, 10 and 1000 while $\alpha = 0.5$, 1 or 2. The solid line represents the time-domain solution and the symbols ●, ▲ and ★ represent the numerical inversion solutions.

that without skin or with a negative skin at the same dimensionless time. The larger dimensionless drawdown in the formation reflects the effect of lower hydraulic conductivity of a positive skin. On the other hand, the smaller dimensionless drawdown reveals the impact of a negative skin with larger conductivity. Fig. 2 indicates that the dimensionless drawdowns for a constant-flux pumping may be divided into three distinct periods, i.e., small time ($\tau < 1$), intermediate time ($1 \leqq \tau \leqq 30$), and large time ($\tau > 30$) if the wellbore skin is presented. This indicates that the dimensionless-drawdown differences between the single-layer and two-layer aquifers are negligible at small- and large-dimensionless times. On the other hand, the observed differences of dimensionless drawdowns are quite large at intermediate-dimensionless time as indicated in Fig. 2 since the relative differences may reach 30% or even higher.

Fig. 3 displays the dimensionless distance-drawdown curves for $\alpha = 0.5$, 1 and 2 when $\tau = 0.1$, 10 or 1000. Within the skin zone ($1 \leqq \rho \leqq 3$), the dimensionless-drawdown differences between the single-layer and two-layer aquifers decrease from the wellbore to the interface of the skin and formation zones. In addition, a larger α yields larger dimensionless drawdown near the wellbore and the dimensionless drawdown for various α increases with τ. In contrast, the dimensionless drawdown with a positive skin is slightly smaller than that without skin (single-layer aquifer) or with a negative skin when $\rho \geqq 3$.

4.2. Effect of skin type

The effect of the skin zone on the drawdown near the well is noteworthy in engineering practice. Fig. 4 depicts the dimensionless time–drawdown curves at the wellbore ($\rho = 1$) when $\alpha = 0.1$, 0.5, 1, 5 or 10. In this figure, the dimensionless drawdown curves for the system with a positive skin are represented by $\alpha = 5$ and 10, and with a negative skin by $\alpha = 0.1$ and 0.5. The dimensionless drawdowns at $\tau = 10$ are respectively 10.03 and 16.01 for $\alpha = 5$ and 10, 1.53 and 2.33 for $\alpha = 0.1$ and 0.5, and 3.30 for $\alpha = 1$. This Indicates that the dimensionless drawdown increases significantly with α values, especially for positive skins. Observed from the dimensionless time–drawdown curves shown in Fig. 4, the dimensionless drawdown is significantly affected by the positive skin than by the negative skin. When an aquifer has a positive skin and is subjected to pumping, the replenishment from the formation is slower because the permeability of a positive skin is smaller than that of the original formation. Thus, the dimensionless drawdown increases quickly with time. In contrast, the change of dimensionless drawdown due to a negative skin is minor because of the larger permeability and faster replenishment from the formation.

Interestingly, the curves plotted in Fig. 4 indicate that the dimensionless drawdown is proportional to the

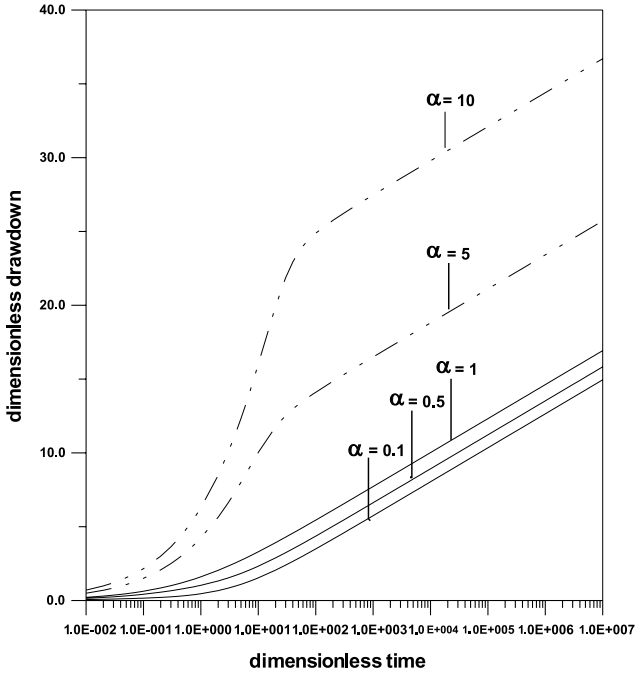

Fig. 4. Dimensionless time–drawdown curves for $\rho = 1$ while $\alpha = 0.1$, 0.5, 1, 5 or 10.

natural logarithm of pumping time when $\tau > 10^2$. This behavior follows Jacob's equation [7], implying that the derived solutions for a two-layer system asymptotically approach Jacob's equation after a long time.

4.3. Effect of skin thickness

This section investigates the effect of skin thickness in the case of a system with a positive skin. The dimensionless time–drawdown curves for $\alpha = 10$ while $\rho = 1$, 3 or 10 are depicted in Fig. 5 to explore the influences of the dimensionless skin thicknesses (e.g., $\rho_1 = 3$ and 10). Note that the dimensionless skin thickness is equal to $\rho_1 - \rho$. Fig. 5 shows that with a smaller dimensionless radial distance (ρ), there is a larger dimensionless drawdown. In addition, the dimensionless drawdown increases with the skin thickness for the same ρ. The well pumping produces a drawdown cone near the well and the hydraulic gradient acts to drive the water flows from the aquifer to the well. Therefore, thicker skin makes aquifer water take more time to flow toward the well and naturally results in larger drawdown near the well.

4.4. Effect of well radius

The effect of the well radius on the dimensionless drawdown due to a constant-flux pumping can be explored by comparing our closed-form solution with the Laplace-domain solution for a point source case presented by Butler [4]. Fig. 6 depicts the dimensionless drawdown curves plotted based on the closed-form solution and Butler's Laplace-domain solution for $\rho_1 = 10$ and $\alpha = 10$ when $\rho = 1$, 5 or 10. The axis of dimensionless time is chosen as $\tau/\rho^2(T_2t/S_2r^2)$, also used in Butler [4], for comparison purposes. The differences of dimensionless drawdowns between these two solutions for $\rho = 1$ are very large when $\tau/\rho^2 = 1$, and small while $\tau/\rho^2 \geqq 1000$. Fig. 6 indicates that if ρ is small then neglecting the effect of well radius may cause significant errors in the drawdown estimation, especially for the case of a large well radius. The dimensionless drawdowns for the aquifer system with and without consideration of the well radius are almost equal when the dimensionless time is large, say $\tau/\rho^2 \geqq 1000$. In reality, both dimensionless drawdown curves approach Jacob's equation at a very long time.

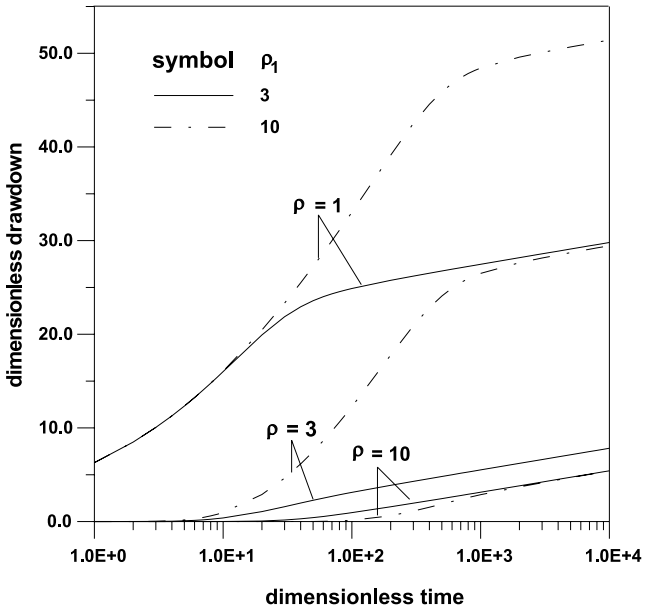

Fig. 5. Dimensionless time–drawdown curves for $\alpha = 10$, and $\rho_1 = 3$ and 10 while $\rho = 1$, 3 or 10.

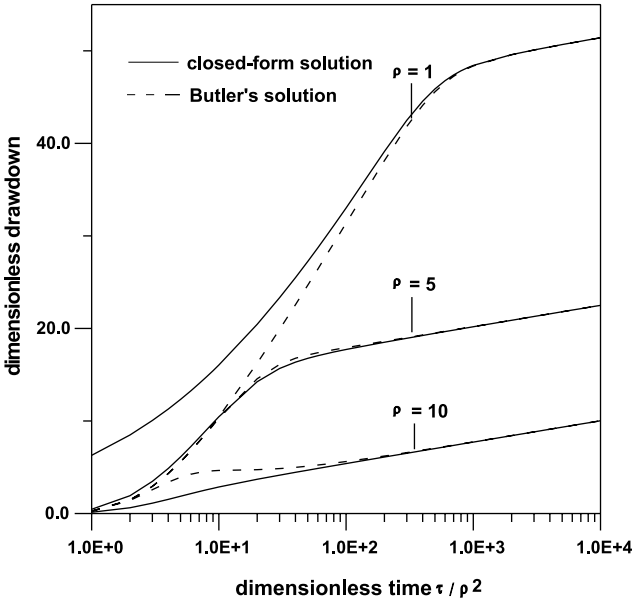

Fig. 6. Comparisons between the closed-form solution and Butler's solution for $\rho_1 = 10$ and $\alpha = 10$ when $\rho = 1$, 5 or 10.

5. Summary and conclusions

An aquifer is considered to be a radial two-layer system if a skin exists near the wellbore. In addition, a patchy aquifer with a well situated at the center of a disc with anomalous properties can also be considered as a radial two-layer system. A mathematical model for an aquifer having a fully penetrating well with a finite-thickness skin and constant-flux pumping is presented. The Laplace-domain solution for the model is derived by the Laplace transforms, and the time-domain solution in terms of the aquifer drawdown is then obtained after taking the Laplace inversion using the Bromwich integral method. A unified numerical method is proposed to efficiently evaluate this solution with accuracy to five decimal places. The values of the time-domain solution evaluated by the proposed approach agree very

well with those of the Laplace-domain solution when numerically inverted by the modified Crump algorithm. These results suggest that both the Laplace-domain solution and the time-domain solution are correctly evaluated. The Laplace-domain solutions for a two-layer aquifer system with a finite-radius well are shown to reduce to those presented by Butler [4] if the well radius is neglected. The estimated drawdowns for a two-layer system are equal to those of the solution for a single-layer system, i.e., $\alpha = \beta = 1$ for a uniform aquifer. Also, the dimensionless drawdown curves plotted for the time-domain solution have been demonstrated to approach the Jacob line for long dimensionless time and distance.

This newly derived solution is used to produce the dimensionless-drawdown curves for investigating the effects of the skin type, the skin thickness, and the well radius on the drawdown distribution. The results show that the differences of dimensionless drawdown between the solutions of the single-layer and two-layer systems are negligible at short and long dimensionless times; however, the differences may reach 30% or even higher at intermediate dimensionless time. On the effect of well radius, the solution for the aquifer system without considering the well radius will yield large errors in estimating dimensionless drawdowns within the skin zone at early time. However, the effect of the well radius on dimensionless drawdown gradually diminishes as the pumping time increases. Thus, the solution for an aquifer system without considering the well radius is applicable only under the conditions of being over a long time, with small well radius, and/or having large skin thickness. Furthermore, the skin thickness also affects the estimated drawdown in an aquifer system. The dimensionless drawdown for a system with a positive skin apparently increases with the skin thickness and decreases with the radial distance.

Acknowledgements

This study was partly supported by the Taiwan National Science Council under Grant no. NSC90-2621-Z-009-003. The authors would also like to thank the three anonymous reviewers for their valuable and constructive comments.

Appendix A. Laplace-domain solution for a point source case

Since $I_1(0) = 0$, the limit of Eq. (8) as r_w approaches 0 becomes

$$\bar{s}_1\Big|_{r_w\to 0} = \frac{Q}{4\pi T_2}\left[\frac{1}{p}\frac{2T_2}{T_1}\frac{\Phi_2 K_0(q_1 r) + \Phi_1 I_0(q_1 r)}{\Phi_2}\right]\lim_{r_w\to 0}\left[\frac{1}{q_1 r_w K_1(q_1 r_w)}\right] \tag{A.1}$$

Carslaw and Jaeger [6, p. 489] gave a formula

$$I_0(z)K_1(z) + K_0(z)I_1(z) = \frac{1}{z} \tag{A.2}$$

The term $\Phi_2 K_0(q_1 r_1) + \Phi_1 I_0(q_1 r_1)$ in the numerator of Eq. (9) reduces to $K_0(q_2 r_1)/(q_1 r_1)$ when applying Eq. (A.2). With $I_1(0) = 0$, the limit of Eq. (9) as r_w approaches 0 becomes

$$\bar{s}_2\Big|_{r_w\to 0} = \frac{Q}{4\pi T_2}\left[\frac{1}{p}\frac{2T_2}{q_1 r_1 T_1}\frac{K_0(q_2 r)}{\Phi_2}\right]\lim_{r_w\to 0}\left[\frac{1}{q_1 r_w K_1(q_1 r_w)}\right] \tag{A.3}$$

Based on $I_0(0) = 1$ and $I_1(0) = 0$, the limit of Eq. (A.2) as z approaches zero becomes

$$\lim_{z\to 0}[zK_1(z)] = 1 \tag{A.4}$$

Accordingly, Eqs. (A.1) and (A.3) respectively reduce to

$$\bar{s}_1\Big|_{r_w\to 0} = \frac{Q}{4\pi T_2}\left[\frac{1}{p}\frac{2T_2}{T_1}\frac{\Phi_2 K_0(q_1 r) - \Phi_1 I_0(q_1 r)}{\Phi_2}\right] \tag{A.5}$$

and

$$\bar{s}_2\Big|_{r_w\to 0} = \frac{Q}{4\pi T_2}\left[\frac{1}{p}\frac{2T_2}{q_1 r_1 T_1}\frac{K_0(q_2 r)}{\Phi_2}\right] \tag{A.6}$$

which is the Laplace-domain solution presented by Butler [4] when neglecting the well radius ($r_w \to 0$). Note that both Eqs. (A.5) and (A.6) were originally given in different form by Barker and Herbert [2], and later slightly revised by Butler [4]; and Eq. (A.6) was also given in Butler and Liu [5, p. 268].

Appendix B. Derivation of Eq. (12)

The convolution theorem [13, p. 63] states that

$$L^{-1}\{f(p)\cdot g(p)\} = \int_0^t F(t-\eta)G(\eta)\,\mathrm{d}\eta \tag{B.1}$$

The inversion of Eq. (8) will lead to the solution of drawdown in a skin zone, thus

$$s_1 = L^{-1}\{\bar{s}_1\} = L^{-1}\{f_1(p)\cdot g_1(p)\} \tag{B.2}$$

Let $f_1(p) = 1/p$ and $g_1(p)$ represent the term on the RHS of Eq. (8) except $1/p$. Applying the Bromwich integral with $L^{-1}\{f_1(p)\} = F(t) = 1$ yields [13, p. 624]

$$G_1(t) = L^{-1}\{g_1(p)\} = \frac{1}{2\pi \mathrm{i}}\int_{\zeta-\mathrm{i}\infty}^{\zeta+\mathrm{i}\infty} \mathrm{e}^{pt} g_1(p)\,\mathrm{d}p \tag{B.3}$$

where p is a complex variable, i is an imaginary unit, and ζ is a large, real, and positive constant so that all the poles lie to the left of the line $(\zeta - \mathrm{i}\infty, \zeta + \mathrm{i}\infty)$.

A single branch point with no singularity (pole) at $p = 0$ exists in the integrand of Eq. (8). Thus, this integration may require using a contour integral for the

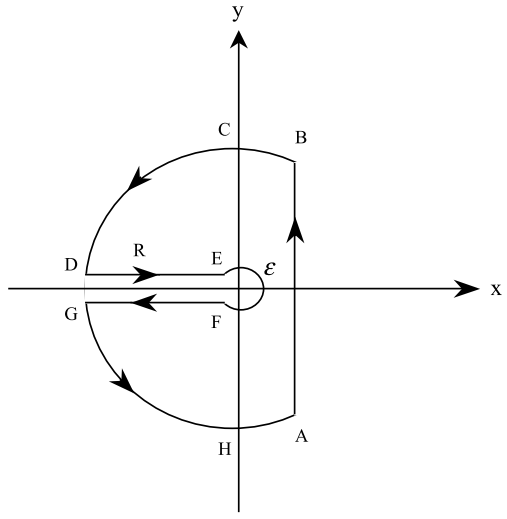

Fig. 7. The closed contour integration of $\bar{s}$ for the Bromwich integral [13].

Laplace inversion. The contour of the integrand is shown in Fig. 7 with a cut of the p plane along a negative real axis, where ε is taken sufficiently small to exclude all poles from the circle about the origin. The closed contour comprises the part AB of the Bromwich line from minus infinity to infinity, semicircles BCD and GHA of radius R, lines DE and FG parallel to the real axis, and a circle EF of radius ε about the origin. Along the small circle EF, the integration around the origin when ε approaches zero is carried out by using the Cauchy integral and the value of integration is equal to zero. The integrals taken along BCD and GHA tend to zero when R approaches infinity. Therefore, Eq. (8) can be superseded by the sum of the integrals along DE and FG. In other words, Eq. (B.3) can be written as

$$G_1(t) = \lim_{\substack{\varepsilon\to 0\\ R\to\infty}} \frac{-1}{2\pi \mathrm{i}} \left[\int_{\mathrm{DE}} \mathrm{e}^{pt} g_1(p)\,\mathrm{d}p + \int_{FG} \mathrm{e}^{pt} g_1(p)\,\mathrm{d}p \right] \tag{B.4}$$

By defining $p = u^2 \mathrm{e}^{-\pi \mathrm{i}} T_1/S_1$, $q_1 = u\mathrm{i}$, and $q_2 = \kappa u \mathrm{i}$, the first term on the RHS of Eq. (B.4) becomes

$$G_{1\mathrm{DE}}(t) = \frac{Q}{2\pi^2 r_\mathrm{w} T_1} \int_0^\infty \mathrm{e}^{-(T_1/S_1)u^2 t} g_1(u) \frac{\mathrm{d}u}{u^2} \tag{B.5}$$

Two formulas give the relationship for the Bessel funtions and the modified Bessel functions [6, p. 490, Eqs. (25) and (26)]

$$K_v\left(z\mathrm{e}^{\pm\frac{1}{2}\pi\mathrm{i}}\right) = \pm\frac{1}{2}\pi\mathrm{i}\,\mathrm{e}^{\mp\frac{1}{2}v\pi\mathrm{i}}[-J_v(z) \pm \mathrm{i}Y_v(z)] \tag{B.6}$$

and

$$I_v\left(z\mathrm{e}^{\pm\frac{1}{2}\pi\mathrm{i}}\right) = \mathrm{e}^{\pm\frac{1}{2}v\pi\mathrm{i}} J_v(z) \tag{B.7}$$

where $v = 0, 1, 2, \ldots$. Based on Eqs (B.6) and (B.7), Eq. (B.5) leads to

$$G_{1\mathrm{DE}}(t) = \frac{Q}{2\pi^2 r_\mathrm{w} T_1} \int_0^\infty \mathrm{e}^{-\frac{T_1}{S_1}u^2 t} \frac{-A_1(u) - \mathrm{i}A_2(u)}{B_1(u) + \mathrm{i}B_2(u)}\,\mathrm{d}u \tag{B.8}$$

where A_1, A_2, B_1 and B_2 were as defined in Eqs. (13)–(16), respectively.

Likewise, by introducing $p = u^2 \mathrm{e}^{\pi\mathrm{i}} T_1/S_1$, $q_1 = -u\mathrm{i}$, and $q_2 = -\kappa u\mathrm{i}$, the integral along FG gives minus the conjugate of Eq. (B.8) as

$$G_{1\mathrm{FG}}(t) = \frac{Q}{2\pi^2 r_\mathrm{w} T_1} \int_0^\infty \mathrm{e}^{-(T_1/S_1)u^2 t} \times \frac{-A_1(u) + \mathrm{i}A_2(u)}{B_1(u) - \mathrm{i}B_2(u)}\,\mathrm{d}u \tag{B.9}$$

The result of the contour integral can then be obtained by combining Eqs. (B.8) and (B.9) as

$$G_1(t) = \frac{Q}{\pi^2 r_\mathrm{w} T_1} \int_0^\infty \mathrm{e}^{-\frac{T_1}{S_1}u^2 t} \times \frac{A_1(u)B_1(u) + A_2(u)B_2(u)}{B_1^2(u) + B_2^2(u)}\,\mathrm{d}u \tag{B.10}$$

Therefore, the complete solution for drawdown distribution in an aquifer with a constant pumping obtained by the convolution is

$$s_1(r,t) = \int_0^t 1 \cdot G_1(\eta)\,\mathrm{d}\eta \tag{B.11}$$

The result of Eq. (B.11) after the integration is

$$s_1 = \frac{Q}{4\pi T_2}\left[\frac{4T_2}{\pi r_\mathrm{w} T_1} \int_0^\infty \left(1 - \mathrm{e}^{-\frac{T_1}{S_1}u^2 t}\right) \times \frac{A_1(u)B_1(u) + A_2(u)B_2(u)}{B_1^2(u) + B_2^2(u)} \frac{\mathrm{d}u}{u^2}\right] \tag{B.12}$$

which is the equation of Eq. (12).

References

[1] Abramowitz M, Stegun IA. Handbook of mathematical functions with formulas, graphs and mathematical tables. In: National Bureau of Standards. Washington: Dover; 1964.
[2] Barker JA, Herbert R. Pumping tests in patchy aquifers. Ground Water 1982;20(2):150–5.
[3] Bixel HC, van Poollen HK. Pressure drawdown and buildup in the presence of radial discontinuities. Soc Petol Eng J 1967:301–9.
[4] Butler Jr JJ. Pumping tests in nonuniform aquifers—the radially symmetric case. J Hydrol 1988;101:15–30.
[5] Butler Jr JJ, Liu WZ. Pumping tests in nonuniform aquifers: the radially asymmetric case. Water Resour Res 1993;29(2):259–69.
[6] Carslaw HS, Jaeger JC. Conduction of heat in solids. 2nd ed. Oxford, UK: Clarendon Press; 1959.
[7] Charbeneau RJ. Groundwater hydraulics and pollutant transport. New York: Prentice-Hall; 2000.
[8] Chu WC, Garcia-Rivera J, Raghaven R. Analysis of interference test data influenced by wellbore storage and skin at the flowing well. J Petol Technol 1980;32:263–9.
[9] Crump KS. Numerical inversion of Laplace transforms using a Fourier series approximation. J Assoc Comput Mach 1976;23(1):89–96.

[10] de Hoog FR, Knight JH, Stokes AN. An improved method for numerical inversion of Laplace transforms. Soc Ind Appl Math J Sci Stat Comput 1982;3(3):357–66.
[11] Hantush MS. Hydraulics of wells. In: Chow VT, editor. Advances in hydroscience. New York: Academic Press; 1964.
[12] Hemker CJ. Transient well flow in vertically heterogeneous aquifers. J Hydrol 1999;22:1–18.
[13] Hildebrand FB. Advanced calculus for applications. 2nd ed. New York: Prentice-Hall; 1976.
[14] Ingersoll LR, Adler FTW, Plass HJ, Ingersoll AG. Theory of earth heat exchangers for the heat pump. Heating, Piping, Air Cond 1950:113–22.
[15] Ingersoll LR, Zobel OJ, Ingersoll AC. Heat conduction with engineering, geological, and other applications. 2nd ed. Madison: University Wisconsin Press; 1954.
[16] International Mathematics and Statistics Library. In: IMSL user's manual, vol. 2. Houston, TX: IMSL; 1987.
[17] Jaeger JC. Heat flow in the region bounded internally by a circular cylinder. Proc Royal Soc Edinburgh 1942;61(Section A):223–8.
[18] Jargon JR. Effect of wellbore storage and wellbore damage at the active well on interference test analysis. J Petrol Technol 1976;28:851–8.
[19] Lebbe LC. Hydraulic parameter identification. Heidelberg: Springer; 1999.
[20] Novakowski KS. A composite analytical model for analysis of pumping tests affected by wellbore storage and finite thickness skin. Water Resour Res 1989;25(9):1937–46.
[21] Novakowski KS. Analysis of aquifer tests conducts in fractured rock: A review of the physical background and the design of a computer program for generating type curves. Ground Water 1990;28(1):99–107.
[22] Papadopulos IS, Cooper Jr HH. Drawdown in a well of large diameter. Water Resour Res 1967;3(1):241–4.
[23] Shanks D. Non-linear transformations of divergent and slowly convergent sequences. J Math Phys 1955;34:1–42.
[24] Stehfest H. Numerical inversion of Laplace transforms. Commun ACM 1970;13(1):47–9.
[25] Streltsova TD. Well testing in heterogeneous formations. New York: John Wiley and Sons; 1988.
[26] Streltsova TD, McKinley RM. Effect of flow time duration on buildup pattern for reservoirs with heterogeneous properties. Soc Petrol Eng J 1984:294–306.
[27] Talbot A. The accurate numerical inversion of Laplace transforms. J Inst Math Appl 1979;23:97–120.
[28] Theis CV. The relation between the lowering of the piezometric surface and the rate and duration of discharge of a well using ground-water storage. Trans Am Geophys Union 1935;16:519–24.
[29] Wikramaratna RS. A new type curve method for the analysis of pumping tests in large-diameter wells. Water Resour Res 1985; 21(2):261–4.
[30] Wynn P. On a device for computing the $e_m(S_n)$ transformation. Math Tables Other Aids Comp 1956;10:91–6.